Numerical Simulation of Binary Black Hole Spacetimes and a Novel Approach to Outer Boundary Conditions

Jennifer Seiler

Ph.D. Thesis Disputation
Leibniz Universität Hannover
February 5, 2010

Outline

Summary of Dissertation

- Numerical evolutions of symmetric and asymmetric binary black hole mergers in to explore the parameter space of binary black hole inspirals:
  - Establish bounds on phenomenological formulae for the final spin and recoil velocity of merged black holes from arbitrary initial data parameters
  - Focus on gravitational-wave emission to quantify how much spin effects contribute to the signal-to-noise ratio and to the relative event rates for the representative ranges in masses and detectors
- Analytical inspiral-merger-ringdown gravitational waveforms from black-hole (BH) binaries with non-precessing spins by matching a post-Newtonian description of the inspiral to our numerical calculations
- Constraint-preserving boundary conditions for the BSSN evolution system
- Well-posed constraint-preserving outer boundary conditions for the Harmonic evolution system . . .

General Relativity and Gravitational Waves

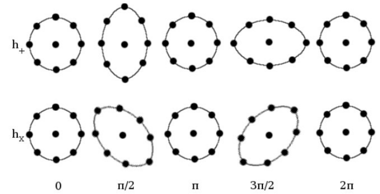

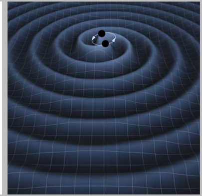

- Coaction between matter and curvature is described by the Einstein Equations:

$$G_{\mu\nu} = 8\pi T_{\mu\nu}$$

- Black holes (BH) = Vacuum ($T_{\mu\nu} = 0$)
- Gravitational Waves (GW) = finite deviation from Minkowski spacetime:

$$g_{\mu\nu} = \eta_{\nu\mu} + h_{\nu\mu}\,, \qquad |h_{\nu\mu}| \ll 1.$$

- Linearized field equations in GR

$$\Box \bar{h}_{\mu\nu} = 16\pi T_{\mu\nu} = (-\partial_t^2 + \nabla^2)\bar{h}_{\mu\nu} = 0.$$

Gravitational waves

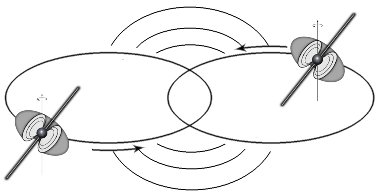

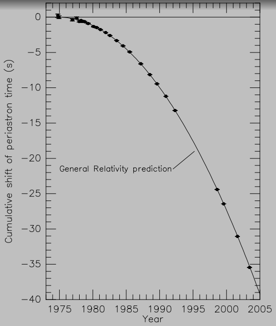

- Gravitational radiation accompanies quadrupolar acceleration of any massive objects as cross-polarized transverse quadrupolar ripples in spacetime will radiate out longitudinally from this system, giving a metric perturbation

$$h_{ij} = h_{+}(e_{+})_{ij} - h_{\times}(e_{\times})_{ij}$$

- Indirect observation: binary pulsar PSR 1913+16
- Hulse-Taylor – Nobel Prize 1993.

Gravitational waves

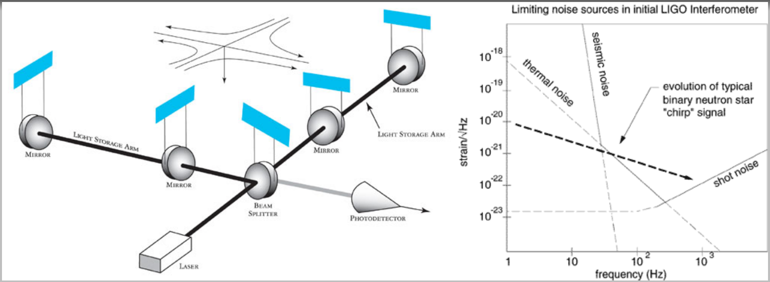

- The coupling between matter and geometry is very weak.

$$R_{\alpha\beta} - \frac{1}{2} R g_{\alpha\beta} = k T_{\alpha\beta}$$

$$k = \frac{8\pi G}{c^4} \simeq 2 \times 10^{-43} \frac{s^2}{m \cdot kg}$$

- Gravitational waves are small features, difficult to detect.
- Unobstructed by intervening matter
- Excellent probe into regions opaque to EM radiation.

Gravitational waves

- Currently there are many ground based detectors online which are designed to detect such passing gravitational waves (LIGO, VIRGO, TAMA, GEO).
- Even for binary black hole inspiral and merger, the signal strength is likely to be much less than the level of any detector noise.
- A technique used for this purpose is *matched filtering*, in which the detector output is cross-correlated with a catalog of theoretically predicted waveforms.
- Therefore, chances of detecting a generic astrophysical signal depend on the size, scope, and accuracy of the theoretical signal template bank.
- The generation of such a template bank requires many models of the GW emitted from compact binary systems.

Binary black holes

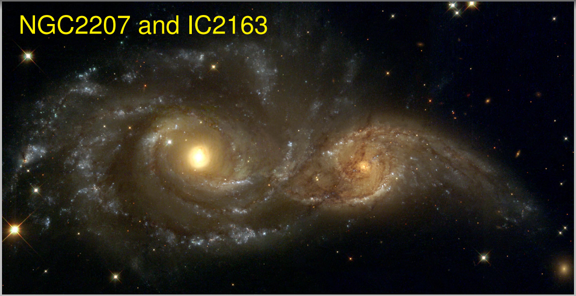

- Optical, radio, and x-ray astronomy have provided us with abundant evidence that many galaxies contain SMBHs in their central nuclei.
- The loudest astrophysical signals in terms of SNR.
- Known examples among galactic binaries.
  - Supermassive – $10^6 - 10^9 M_\odot$.
  - Low frequency sources – space-based detector (LISA)
- Formation processes for stellar mass binaries:
  - Collapse within a binary neutron star system.
  - Capture within a dense region, eg. globular cluster.

Binary black holes

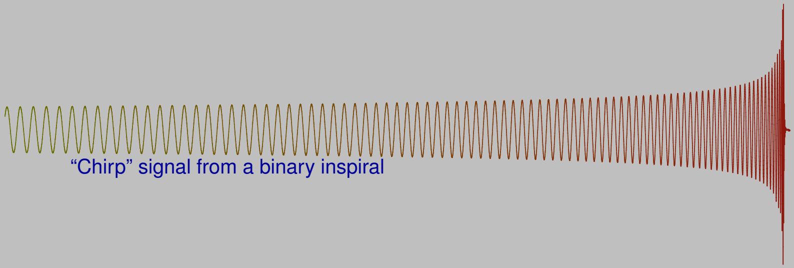

- Black holes captured → highly elliptical orbits.
- Radiation of gravitational energy
  → circularisation of orbits. → *inspiral* (PN)
- Decay of orbit leading to
  →*plunge* (NR) → *merger* (NR)
- Single perturbed BH remnant
  → exponential *ringdown* to axisymmetric (Kerr) BH.

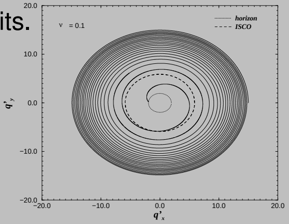

Numerical Relativity

$$R_{\alpha\beta} - \frac{1}{2} g_{\alpha\beta} R = 8\pi T_{\alpha\beta}$$

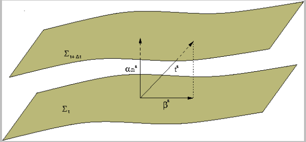

- The Einstein equations are a hyperbolic set of nonlinear wave equations for the geometry
- As such, they are most conveniently solved as an initial-boundary-value problem:
  - Assume the geometry is known at some initial time t_0.
  - Evolve the data using the Einstein equations.
  - Prescribe consistent boundary conditions at some finite radius r_0.
- Geometry specified on an initial data slice:
  - metric g_{ab} specifies the intrinsic geometry of the slice.
  - extrinsic curvature determines the embedding in 4D space.
- Evolution equations are integrated using standard numerical methods, eg. Runge-Kutta.
- The equations are differentiated in space on a discrete computational grid using finite differencing methods

Finite Differencing

- discretize our continuum intial data and solve the spatial derivatives in our PDEs.

$$x_i = (i - \frac{1}{2})h_x \,, \qquad 0 \leq i \leq N_x \,,$$

- finite difference approach using Taylor series expansions

$$\begin{aligned} f(x+h) &= f(x) + h\frac{df}{dx}|_x + \frac{h^2}{2}\frac{d^2 f}{dx^2}|_x + \frac{h^3}{6}\frac{d^3 f}{dx^3}|_x + \ldots \\ f(x-h) &= f(x) - h\frac{df}{dx}|_x - \frac{h^2}{2}\frac{d^2 f}{dx^2}|_x - \frac{h^3}{6}\frac{d^3 f}{dx^3}|_x + \ldots \\ \frac{df}{dx} &= \frac{f(x+h) - f(x-h)}{2h} - \frac{1}{6}f'''(\zeta)h^2 \,, \end{aligned}$$

- Fourth order:

$$\frac{df}{dx} = \frac{-f(x+2h) + 8f(x+h) - 8f(x-h) + f(x-2h)}{12h}$$

- replace PDE with an algebraic equation on a discrete grid

Method of Lines

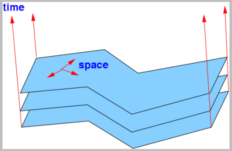

- FD the spatial derivatives of the PDE leaving the time derivatives continuous.
- This leads to a coupled set of ODEs for the time dependence of the variables $u = (u_{ij})$ at the spatial grid points,

$$\partial_t u = f(t, u)$$

- ODE integrator to integrate these ODEs forward in time.

$$\| u^{n+1} - u^n \| = \mathcal{O}(\Delta t^{p+1})$$

Complications of Numerical Relativity

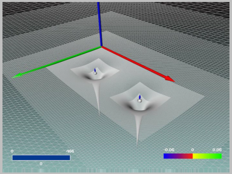

- The initial-boundary-value problem needs to be well-posed.
  - Choice of geometrical variables $\longrightarrow$ strongly hyperbolic evolution system.
- Evolution of the coordinates needs to be carefully considered.
- The BH centers are physical singularities:
  - Treated as “punctures” by choice of gauge.
  - Excised by imposing a boundary condition around the singularity.
- It is only within the last 5 years that this problem has been solved:
  - Pretorius (2005), Campanelli et al. (2005), Baker et al. (2005).

Einstein equations in 3+1 form

The Einstein equations are manifestly covariant

- Need to reformulate as a *Cauchy problem*
- We have ten equations and ten independent components of the four metric $g_{\mu\nu}$, the same number of equations as unknowns.
- Only six of these ten equations involve second time-derivatives of the metric.
- The other four equations, thus, are not evolutions equations. We call these our *constraint equations*.

There are a number of non-unique aspects of the 3+1 decomposition

- Choice of evolution variables
- Choice of gauge
- Binary black hole codes currently use either a harmonic formulation, or a modified (“conformal traceless” or “BSSN”) ADM system.

Coordinate conditions

There are a number of features we'd like to see in a good choice of coordinates:

- Cover regions of spacetime of interest
  - Also some geometric criteria: Preserve volume elements, prevent shear, avoid caustics.
- Simplify equations of motion
  - eliminate evolution variables
  - recast equations into nice form (eg. harmonic coords)
- Simplify the physics (eg. reduce dynamics on the numerical grid)
  - minimal distortion (Smarr-York 1978), "symmetry seeking" (Garfinkle-Gundlach 1999)
  - known asymptotic states
- Avoid physical singularities
- Computationally efficient
- Compatible with hyperbolicity, well-posedness

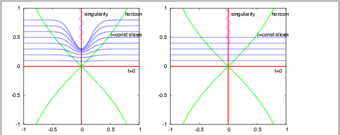

Hyperbolic formulations

- The 3+1 Einstein evolution equations can be written symbolically in the form:

$$\partial_t \mathbf{u} + \mathbf{A}^i \partial_i \mathbf{u} = \mathbf{s}(\mathbf{u})$$

- Propagation of characteristics is determined by eigenvalues of $\mathbf{A}$.
  - This is significant, among other things, for the numerical Courant-Friedrich-Levy (CFL) condition, and setting boundary conditions.
- The system is strongly hyperbolic if $\mathbf{A}$ has real eigenvalues and is diagonalizable.
- The initial value problem is well-posed if and only if $\mathbf{A}$ has a complete set of eigenvalues.
- A stable numerical scheme can only be implemented for well-posed systems.

Reduction to explicitly hyperbolic form

- Expanding

$$R_{\alpha\beta} = 0,$$

we get a PDE whose principle part contains mixed 2nd-derivatives of the metric:

$$-\frac{1}{2}\Box g_{ab} - \frac{1}{2}g^{ij}\left(g_{ij,ab} - g_{ia,bj} - g_{ib,aj}\right) + g^{ij}\left({\Gamma^k}_{ai}\Gamma_{jkb} - {\Gamma^k}_{ab}\Gamma_{ijk}\right) = 0.$$

- Harmonic gauge: Mixed 2nd derivatives can be removed by introducing the new variables $-{g^{ai}}_{,i} = \Gamma^a$:

$$\Box g_{ab} = 2g_{i(a}\partial_{b)}\Gamma^i + 2\Gamma^i\Gamma_{(ab)i} + 2g^{ij}\left(2{\Gamma^k}_{i(a}\Gamma_{b)kj} + {\Gamma^k}_{ai}\Gamma_{kjb}\right)$$

- The Einstein equations are explicitly in the form of a 2nd order wave equation for the metric.

"Generalised" Harmonic Coordinates

Coordinates:

- GH coordinates, x^μ, satisfy the condition $\Box x^\mu = \Gamma^\mu = F^\mu$.
- $F^\mu(g^{\alpha\beta}, x^\rho)$ as a source function chosen to fine tune gauge to address the requirements of specific simulations.
- Provides solutions of the EEs provided that the constraints:

$$C^\mu \equiv \Gamma^\mu - \widehat{\Gamma}^\mu = \frac{1}{\sqrt{-g}} \frac{\partial}{\partial x^\kappa} \left(\sqrt{-g} g^{\lambda\kappa} \right) - \widehat{\Gamma}^\mu = 0$$

and their time derivatives are initially satisfied.

Evolution Variables:

- We define the evolution variables $\tilde{g}^{\mu\nu} \equiv \sqrt{-g} g^{\mu\nu}$ and $Q^{\mu\nu} \equiv n^\rho \partial_\rho \tilde{g}^{\alpha\beta}$, where n^ρ is timelike.
- This simplifies the constraint equations to

$$C^\mu \equiv -\frac{1}{\sqrt{-g}} \partial_\alpha \tilde{g}^{\alpha\mu} - \widehat{\Gamma}^\mu$$

and gives us a first order in time evolution system.

Harmonic coordinates

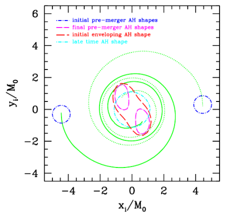

- Hyperbolicity, and thus stability, follows directly from the reduction to harmonic form.
- The harmonic reformulation comes at the price of introducing 4 new variables:

$$\Gamma^{\alpha} := -\partial_{\beta} g^{\alpha\beta}.$$

- These are evolved independently of the metric, thus we have new constraints which must be satisfied by any numerical scheme:

$$\Gamma^{\alpha} + \partial_{\beta} g^{\alpha\beta} = 0.$$

- The first stable evolution of a binary black hole system used harmonic coordinates [Pretorius 2005].

The AEIHarmonic Code

- Generalized harmonic system
- 2nd differential order in space
- Constraint damping
- 4th order finite differencing
- Moving lego-excision
- Mesh refinement (with Carpet)
- Written for the Cactus Computational Toolkit
- 4th order Runga Kutta Time integration

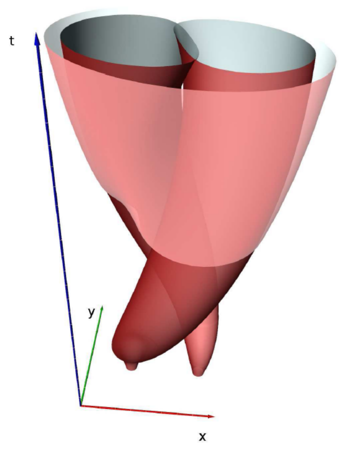

Inspiral and Merger with Harmonic Coordinates. A smooth crossing of the horizons can clearly be seen.

The Initial Boundary Value Problem

- To simulate spacetimes numerically on a finite grid we truncate the computational domain by introducing an artificial outer boundary.
- The boundary conditions should:
  - be compatible with the constraints
  - reduce reflections
  - yield a well-posed initial-boundary value problem.

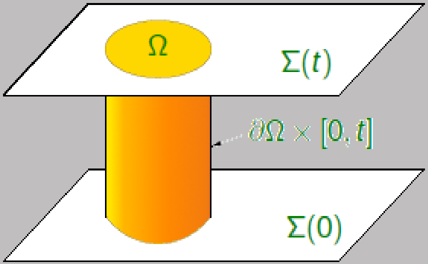

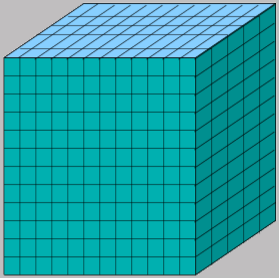

Summation by Parts Boundaries

- The SBP method allows us to derive difference operators and boundary conditions which control the energy growth of the system and thus provide a mathematically and numerically well-posed system.
- A discrete difference operator is said to satisfy SBP for a scalar product $\langle u, v \rangle$ if the property

$$\langle u, Dv \rangle + \langle v, Du \rangle = (u \cdot v) \big|_a^b$$

  holds for all functions u, v in $[a, b]$.
- One can construct a 3D SBP operator by applying the 1D operator to each direction. The resulting operator also satisfies SBP with respect to a diagonal scalar product

$$(u, v)_\Sigma = h_x h_y h_z \sum_{ijk} \sigma_{ijk} u_{ijk} \cdot v_{ijk},$$

- Using SBP difference operators we can formulate an energy estimate for our evolution system...

SBP Operators

- constructing finite difference stencils D of a given order, τ, such that

$$Du = \frac{du}{dx} + \mathcal{O}(h^{\tau}),$$

  and which satisfy the SBP property.
- determined up to the boundaries by solving the set of polynomials

$$Dx^m - \frac{dx^m}{dx} = 0, \qquad m = 0, 1, \ldots, \tau,$$

  which establish the order of accuracy τ of the approximation.
- The SBP rule provides an additional set of restrictions,

$$\begin{aligned} \langle u, Du \rangle &= -\frac{1}{2} u^2(0)\,, \\ \langle u+v, D\,(u+v) \rangle_h &= \langle D\,(u+v)\,, u+v \rangle_h - (u_0+v_0)^2\ , \end{aligned}$$

Well-Posed Boundaries

- The use of SAT ('penalty') allows us to choose values for the free parameters in the boundary terms which conserve the energy in the system.

$$\begin{aligned}\partial_t Q^{\mu\nu} &= -\frac{\gamma^{it}}{\gamma^{tt}} D_{i+} Q^{\mu\nu} - (\gamma^{ij} + \frac{\gamma^{it}\gamma^{jt}}{\gamma^{tt}}) H^{-1}(A_{ij} + (E_0 - E_N) S_i)\gamma^{\mu\nu} + \tilde{S} \\ &+ \tau_{0_i} H^{-1} E_{0_i}(\alpha_{0_i} g_t^{\mu\nu} + \beta_{0_i} S_i g^{\mu\nu} + \gamma_{0_i} g^{\mu\nu} - e_{0_i} g_0) \\ &+ \tau_{N_i} H^{-1} E_{N_i}(\alpha_{N_i} g_t^{\mu\nu} + \beta_{N_i} S_i g^{\mu\nu} + \gamma_{N_i} g^{\mu\nu} - e_{N_i} g_N)\end{aligned}$$

- I determine the time dependence of the energy for this system with these penalties in order to derive coefficients for my penalty terms at the boundary points.

$$\frac{d}{dt}\left(\|u_t\|^2 + \|-\frac{\gamma^{ij}}{\gamma^{tt}} u_i u_j\|\right) = (\langle u_t, u_{tt}\rangle + \langle u_{tt}, u_t\rangle) - \frac{\gamma^{ij}}{\gamma^{tt}}(\langle u_i, u_{jt}\rangle + \langle u_{it}, u_j\rangle)$$

Well-Posed Boundaries

- I solve for this dependence by the SBP rule and substituting in the boundary conditions.

$$(\partial_t - \partial_x)\left[r^2\left(g^{\mu\nu} - g_0^{\mu\nu}\right)\right] = 0$$

- we solve for the coefficients then by enforcing maximally dissipative boundaries.
- This gives a well-posed semi-discrete system by placing a bound on the energy growth of the system.

$$\begin{aligned}
\partial_t Q^{\mu\nu} \quad = \quad & -\frac{\gamma^{it}}{\gamma^{tt}} D_{i+} Q^{\mu\nu} - (\gamma^{ij} + \frac{\gamma^{it}\gamma^{jt}}{\gamma^{tt}}) H^{-1}(A_{ij} + (E_0 - E_N)S_i)\gamma^{\mu\nu} \\
+ \quad & \frac{2\gamma^{ij}}{\gamma^{tt}\beta_0} H^{-1} E_{0_i}[(1 + \frac{\gamma^{it}}{\gamma^{tt}}) D_{i+}\gamma^{\mu\nu} - \frac{Q^{\mu\nu}}{\gamma^{tt}} + \frac{2x}{r^2}(\gamma^{\mu\nu} - g_0)] \\
+ \quad & \frac{2\gamma^{ij}}{\gamma^{tt}\beta_N} H^{-1} E_{N_i}[(1 - \frac{\gamma^{it}}{\gamma^{tt}}) D_{i+}\gamma^{\mu\nu} + \frac{Q^{\mu\nu}}{\gamma^{tt}} + \frac{2x}{r^2}(\gamma^{\mu\nu} - g_N)]
\end{aligned}$$

Constraint Preservation

- Sommerfeld-type outgoing conditions:

$$\left(\partial_t - \partial_x - \frac{1}{r}\right)\left(\gamma^{\mu\nu} - \gamma_0^{\mu\nu}\right) = 0$$

- For CP Boundaries we set the four $\gamma^{t\mu}$ from the constraints:

$$C^\mu = -\partial_t \gamma^{t\mu} - \partial_i \gamma^{i\mu} - F^\mu = 0$$

and we derive a set of outgoing conditions which specify the other 6 metric components:

$$\left(\partial_x + \partial_t + \frac{1}{r}\right)\left(\gamma^{AB} - \gamma_0^{AB}\right) = 0$$

$$\left(\partial_x + \partial_t + \frac{1}{r}\right)\left(\gamma^{tA} - \gamma^{xA} - \gamma_0^{tA} + \gamma_0^{xA}\right) = 0$$

$$\left(\partial_x + \partial_t + \frac{1}{r}\right)\left(\gamma^{tt} - 2\gamma^{xt} + \gamma^{xx} - \gamma_0^{tt} + 2\gamma_0^{xt} - \gamma_0^{xx}\right) = 0$$

- which additionally gives us a bound on the constraint growth see: {Kreiss and Winicour, gr-qc 0602051}

Test Waves

- Shifted scalar waves
  - Linear waves with shift $\beta^i = g^{it}/g^{tt}$:

$$\left(\partial_t^2 - 2\beta^i\partial_i\partial_t - \left(\delta^{ij} - \beta^i\beta^j\right)\partial_i\partial_j\right)\phi = 0\,,$$

- Teukolsky waves
  - Quadrupole wave solutions to the linearized Einstein equations:

$$\begin{aligned} ds^2 &= -dt^2 + (1 + Af_{rr})dr^2 + (Bf_{r\phi})rdrd\theta + (Bf_{r\theta})r\sin\theta drd\phi + (1 + Cf^{(1)}_{\theta\theta} + Af^{(2)}_{\theta\theta})r^2 d\theta^2 \\ &+ [2(A - 2C)f_{\theta\phi}]r^2\sin\theta d\theta d\phi + (1 + Cf^{(1)}_{\phi\phi} + Af^{(2)}_{\phi\phi})r^2\sin^2\theta d\phi^2\,. \end{aligned}$$

- Brill waves
  - Asymmetric non-linear waves: the initial spatial metric takes the form

$$ds^2 = \Psi^4[e^{2q}(d\rho^2 + dz^2) + \rho^2 d\phi^2],$$

in cylindrical (ρ, ϕ, z) coordinates. I choose q of the form of a Gaussian packet centered at the origin,

$$q = a\rho^2 e^{-r^2},$$

Stringent Tests

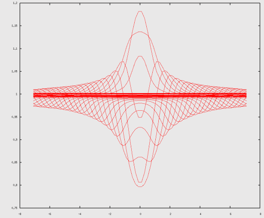

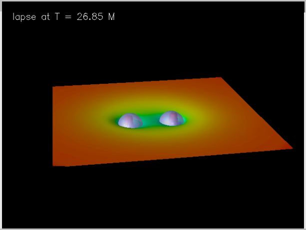

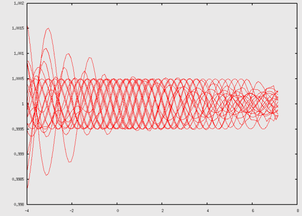

- Convergence tests
  - 2D Shifted gauge wave test
  - known exact solution
- Stability tests
  - Brill with random noise
  - Brill with checkerboard
- Black holes
  - Perturbed Schwarzschild
  - Head-on collision of equal mass black holes

Results for High Shifts

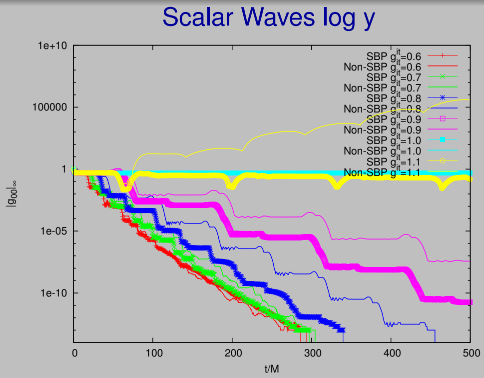

- Tests with shifted scalar wave testbed
- Stability test for various shifts ($0.6 < \beta^i < 1.1$):

$$\left(\partial_t^2 - 2\beta^i \partial_i \partial_t - \left(\delta^{ij} - \beta^i \beta^j\right) \partial_i \partial_j\right) \phi = 0 \,,$$

- Thin = Standard Sommerfeld, Thick = SBP
- SBP stable for superluminal shifts

Results for High Shifts

Scalar Waves no log

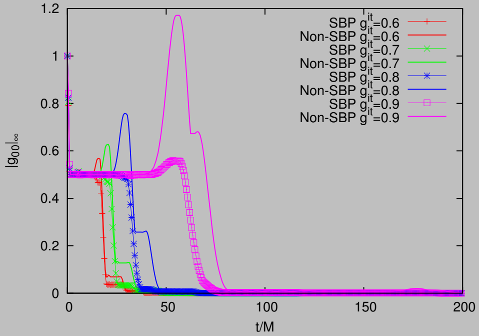

- Tests with shifted scalar wave testbed
- Stability test for various shifts ($0.6 < \beta^i < 1.1$):
- Thin = Standard Sommerfeld, Thick = SBP
- Reflections for standard BCs clearly visible for naive boundaries, reflect back and forth hence the stepping

Robust Stability Tests

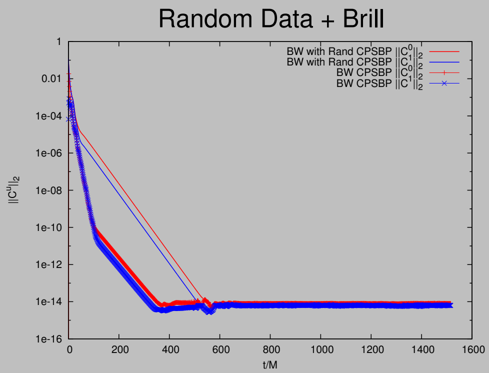

- Random Data + Brill Wave
  - Random Kernel Amplitude $= 0.1$
  - Brill Wave Amplitude $= 0.5$
  - $dx = 0.2\,,\; xmax = 7.1$
- Runs stable for in nonlinear regime for Brill Waves.
- Stable for random data
- Standard Sommerfeld type breaks rapidly for this simulation

Robust Stability Tests

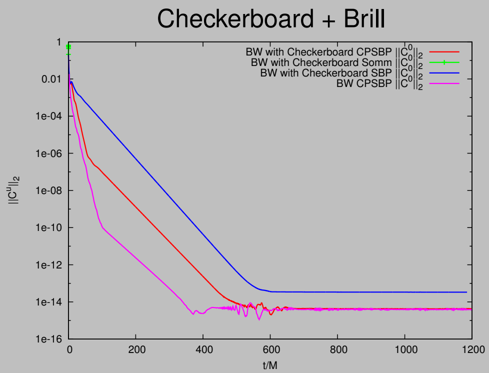

- Checkerboard Data + Brill Wave
  - for each $x(i), y(j), z(k)$ we add $(-1)^{i+j+k}A$ highest frequency noise possible
  - Checker Kernel $A = \pm 0.2$
  - Brill Wave Amplitude $= 0.5$
  - $dx = 0.2$, $xmax = 7.1$
- Standard Sommerfeld seen in green (breaks quickly)

Results for Teukolsky Waves

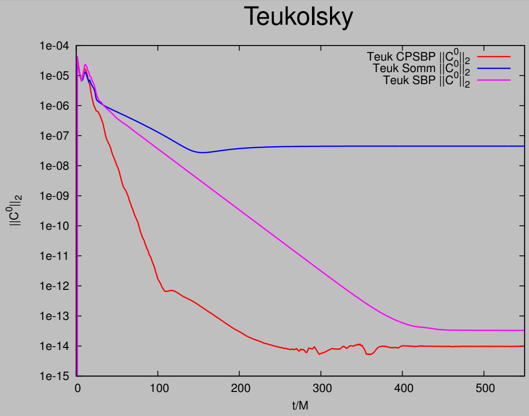

- Constraint Norms for runs with high amplitude Teukolsky Waves:
  - CP 'SBP' = Red, SBP = Magenta
  - Standard Sommerfeld-type = Blue
- Boundaries at $7.1M$, amplitude 0.001

Results for Schwarzschild Runs

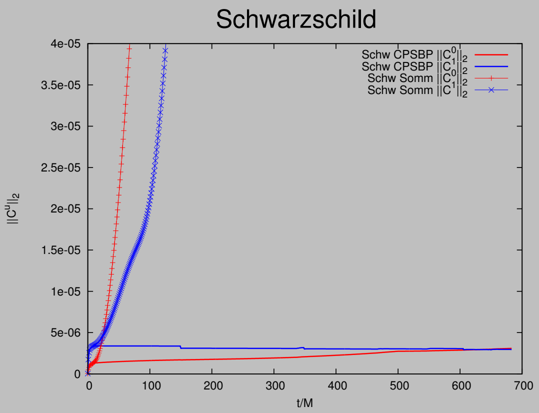

- Schwarzschild run with boundaries too close in (40 M) for sommerfeld-type boundaries
- CPSBP remains stable

Shifted Gauge Wave Convergence Test

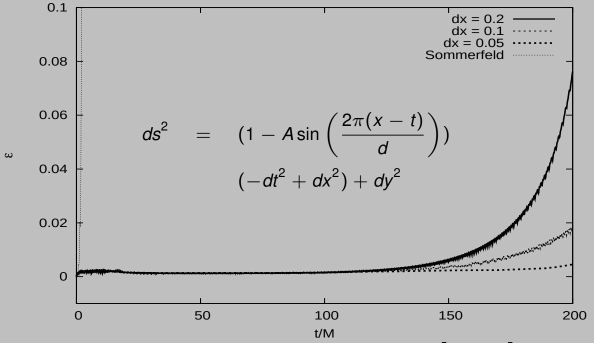

- $A = 0.01$, $d = 2$, and boundary width $x, y \in [-7, 7]$.
- $dx, dy = 0.05, 0.1, 0.2$ with the error $\mathcal{E} = \| \Phi_\rho - \Phi_{exact} \|_\infty$
- convergence rates

$$r(t) = \log_2\left(\frac{\| \Phi_{h=2\delta x} - \Phi_{exact} \|_\infty}{\| \Phi_{h=\delta x} - \Phi_{exact} \|_\infty}\right),$$

$r(t = 10)_{(0.05.0.1)} = 4.0380$, $r(t = 30)_{(0.05.0.1)} = 3.3907$, and $r(t = 200)_{(0.1.0.2)} = 2.0457$.

Head-on Runs with CPSBP

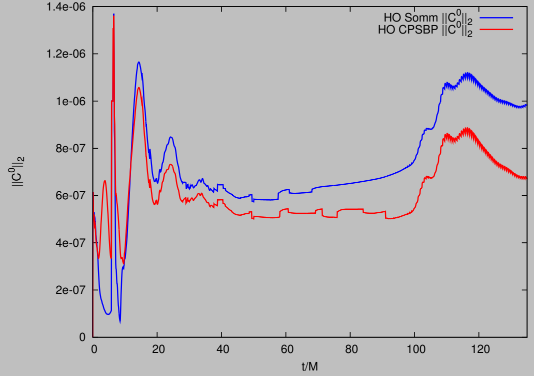

- Head-on Collision (mass 0.5, 2.5 M separation)
- L2 Norm of Constraints for CPSBP vs regular boundaries
- Significant improvement in constraint preservation
- Circumference ratios almost identical
- Some boundary effects are visible for the standard BC runs which are not in the CPSBP run

Conclusions

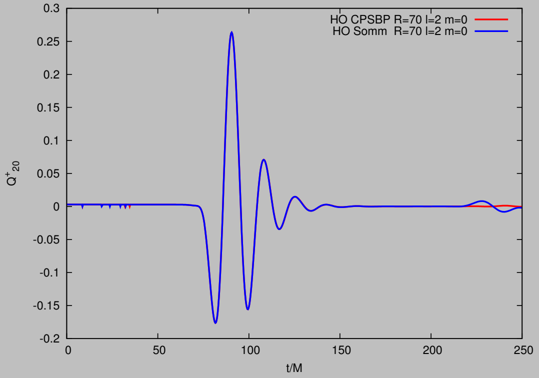

- provides a provably well-posed and demonstrably stable IBVP for Generalized Harmonic evolutions on a Cartesian grid
- Stands up to stability tests
- We have developed a method which allows us to consistently use SBP on a Cartesian grid for corners and edges, and for a 2nd order in space system

Publications

- L. Rezzolla, P. Diener, E. N. Dorband, D. Pollney, C. Reisswig, E. Schnetter, JS. **The Final Spin From the Coalescence of Aligned-spin Black-hole Binaries**. *Astrophys. J.* **674** *(2008) L29*. Preprint: arXiv.org:0710.3345 [gr-qc]
- L. Rezzolla, E. Barausse, E. N. Dorband, D. Pollney, C. Reisswig, JS, S. Husa. **On the final spin from the coalescence of two black holes**. *Phys. Rev. D* **78** *(2008) 044002*. Preprint: arXiv:0712.3541[gr-qc]
- JS, B. Szilagyi, D. Pollney. **Constraint Preserving Boundaries for a Generalized Harmonic Evolution Systems**. *Class. Quant. Grav.* **25** *(2008) 175020*. Preprint: arXiv:0802.3341 [gr-qc]
- B. Aylott, *et al.* (including JS). **Testing gravitational-wave searches with numerical relativity waveforms: Results from the first Numerical INJection Analysis (NINJA) project**. *Classical and Quantum Gravity* **26**, *(2009) 165008*. Preprint: arXiv:0901.4399 [gr-qc]
- B. Aylott, *et al.* (including JS). **Status of NINJA: the Numerical INJection Analysis project** *Classical and Quantum Gravity* **26**, *(2009) 114008*. Preprint: arXiv:0905.4227 [gr-qc]
- C. Reisswig, S. Husa, L. Rezzolla, E. Dorband, D. Pollney, JS. **Gravitational-wave detectability of equal-mass black-hole binaries with aligned spins**.*Phys. Rev. D* **80**, *(2009) 124026* . Preprint: arXiv:0907.0462 [gr-qc]
- P. Ajith, *et al.* (including JS). **“Complete” gravitational-waveforms for black-hole binaries with non-precessing spins**. Preprint: arXiv:0909.2867 [gr-qc]

Parameter studies with spinning black holes

Aligned spin leads to an orbital hangup.

r0	r1	r2	r3	r4	r5	r6	r7	r8

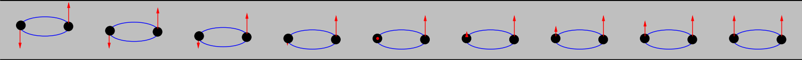

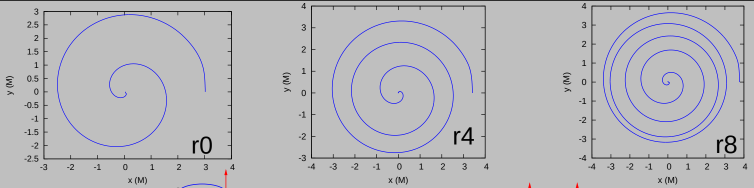

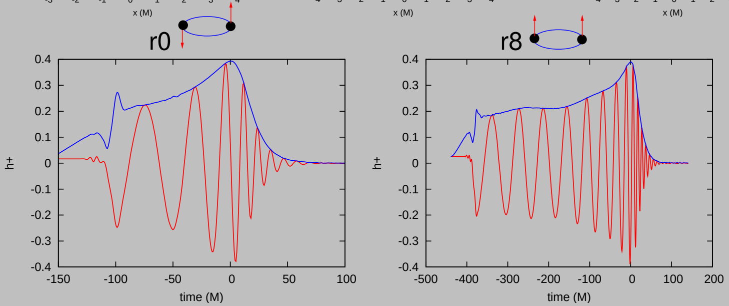

Kicks

- For an equal-mass, non-spinning binary merger, the remnant will be a stationary, spinning black hole.
- If an asymmetry in the bodies is present, the emitted in gravitational waves will also have asymmetry.
- As a result, the remnant black hole will have momentum relative to distant stationary observers, called a recoil or kick.
- Asymmetries in the emitted gravitational wave energy are a result of:
    - Unequal masses.
    - Unequal spin magnitudes.
    - Spins which are misaligned with each other or the orbital angular momentum.

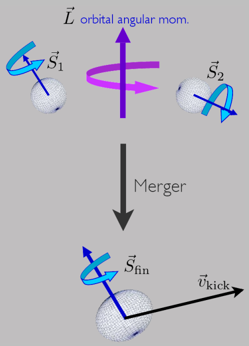

Black hole kicks

- The recoil results from couplings of various wave modes, which are integrated over the entire inspiral time.

$$\mathcal{F}_i \equiv \dot{P}_i = \frac{r^2}{16\pi} \int d\Omega\, n_i \left(\dot{h}_+^2 + \dot{h}_\times^2\right)$$

- PN (2.5) suggests a linear increase of recoil with spin ratio:

$$|v|_{\rm kick} = c_1 \frac{q^2(1-q)}{(1+q)^5} + c_2 \frac{a_2 q^2(1-qa_1/a_2)}{(1+q)^5} = \tilde{c}_2 a_2 \left(1 - \frac{a_1}{a_2}\right)$$

- In fact, the numerical data points to a quadratic dependence:

$$|v|_{\rm kick} = a_2(c_1 - c_2(\frac{a_1}{a_2}) + c_3(\frac{a_1}{a_2})^2)$$

- The maximum recoil for the anti-aligned case:

$$|v|_{\rm kick} = 448 \pm 5 km/s$$

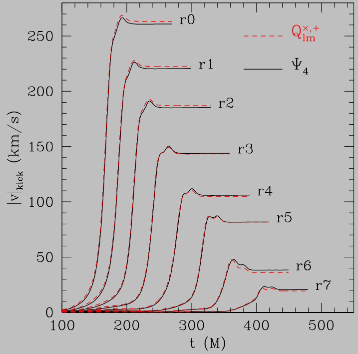

Recoil velocities

- The recoil velocity of the final BH can be fit to a quadratic function of the initial BH spins (a_1, a_2):

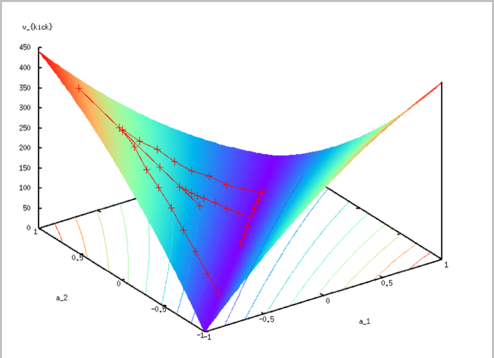

$$|v_{\text{kick}}| = |c_1(a_1 - a_2) + c_2(a_1^2 - a_2^2)| \,.$$

$$c_1 = -220.97 \pm 0.78 \,, \qquad c_2 = 45.52 \pm 2.99$$

Zero kick when $a_1 = a_2$ Linear scaling along $a_1 = -a_2$

Spins

- Equation to predict final spin of merged black hole

$$|a_{\mathrm{fin}}| = \frac{1}{(1+q)^2}\Big[|a_1|^2 + |a_2|^2 q^4 + 2|a_2||a_1|q^2\cos\alpha + 2\left(|a_1|\cos\beta + |a_2|q^2\cos\gamma\right)|\ell|q + |\ell|^2 q^2\Big]^{1/2},$$

where $\cos\alpha \equiv \hat{a}_1 \cdot \hat{a}_2$, $\cos\beta \equiv \hat{a}_1 \cdot \hat{\ell}$, $\cos\gamma \equiv \hat{a}_2 \cdot \hat{\ell}$.

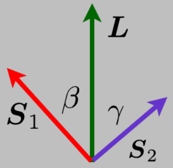

- In order to obtain $|\ell|$ we need to match this equation against general second order polynomial expansions for:
  - Equal mass, unequal but aligned spin binaries
  - Unequal mass, equal spin binaries

$$|\ell| = \frac{s_4}{(1+q^2)^2}\left(|a_1|^2 + |a_2|^2 q^4 + 2|a_1||a_2|q^2\cos\alpha\right) + \left(\frac{s_5\nu + t_0 + 2}{1+q^2}\right)\left(|a_1|\cos\beta + |a_2|q^2\cos\gamma\right) + 2\sqrt{3} + t_2\nu + t_3\nu^2 .$$

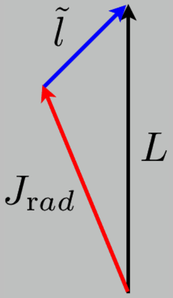

  - Numerical simulations to obtain s_4, s_5, t_0, t_2, t_3.
  - Test against generic misaligned spin binaries.

Unequal Mass, Aligned Spins

- The spin of the final black hole has been determined for very generic initial conditions:
  - Arbitrary aligned spins
  - Unequal masses
- In the extreme-mass-ratio limit, approximation methods can be used.

$$a_{\rm fin} = a + s_4 a^2 \nu + s_5 a \nu^2 + t_0 a \nu + 2\sqrt{3}\nu + t_2 \nu^2 + t_3 \nu^3$$

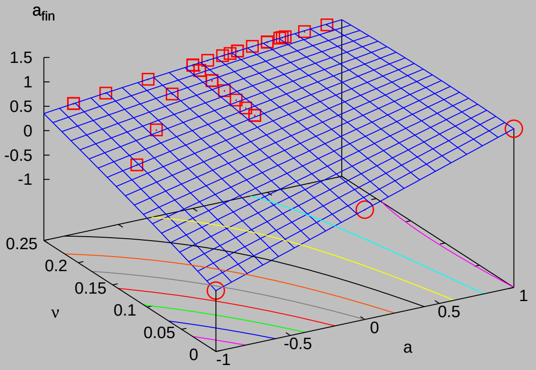

$$s_4 = -0.129 \pm 0.012$$
$$s_5 = -0.384 \pm 0.261$$
$$t_0 = -2.686 \pm 0.065$$
$$t_2 = -3.454 \pm 0.132$$
$$t_3 = 2.353 \pm 0.548$$

Detection

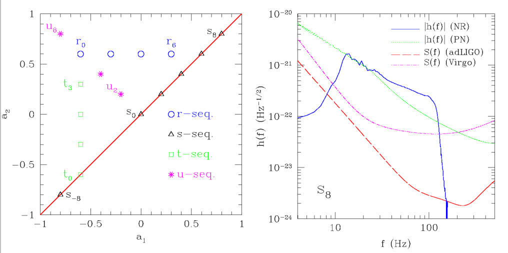

- Each of these binaries and across a set of different masses we calculate the signal-to-noise ratio (SNR) for the LIGO, enhanced LIGO (eLIGO), advanced LIGO (AdLIGO), Virgo, advanced Virgo (AdVirgo), and LISA detectors.

$$\rho_{\rm avg} = \frac{1}{\pi} \sum_{\ell m} \int df \frac{|\tilde{h}_{\ell m}(f)|^2}{S_h(f)} \,.$$

  $S_h(f)$ is the noise power spectral density for a given detector.
- Equal-spin binaries with maximum spin aligned are more than “three times as loud” as the corresponding binaries with anti-aligned spins, thus corresponding to event rates up to 27 times larger.
- Energy radiated in gravitational waves always have efficiencies $E_{\rm rad}/M \gtrsim 3.6\%$, which can become as large as $E_{\rm rad}/M \simeq 10\%$ for maximally spinning binaries.

Detection

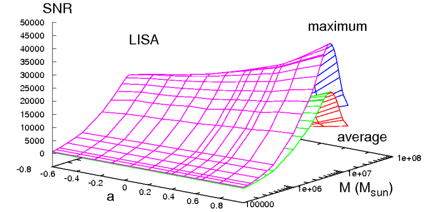

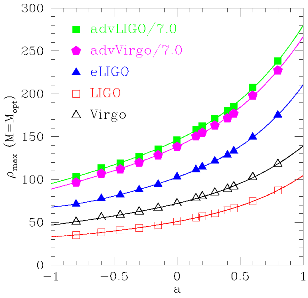

- For any value of a, the maximum horizon distance/SNR also marks the "optimal mass" for the binary $M_{\rm opt}$.
- For any mass, the SNR can be described with a low-order polynomial of the initial spins $\rho = \rho(a_1, a_2)$ and generally it increases with the total dimensionless spin along the angular momentum direction, $a \equiv \frac{1}{2}(\boldsymbol{a}_1 + \boldsymbol{a}_2) \cdot \hat{\boldsymbol{L}}$.
- Higher-order contributions in the waveforms with $\ell \leq 4$ for low masses $M \in [20, 100]$ they contribute, say for the LIGO detector, $\approx 2.5\%$, whereas for intermediate masses $M > 100\ M_\odot$ they

Distinguisability

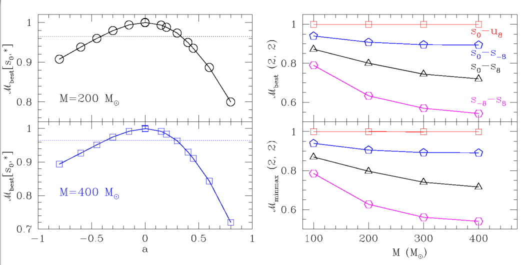

- The match between two waveforms $h_1(t)$ and $h_2(t)$ can be calculated via the weighted scalar product

$$\langle h_1 | h_2 \rangle = 4\Re \int_0^\infty df \, \frac{\tilde{h}_1(f)\tilde{h}_2^*(f)}{S_h(f)} \, .$$

- The overlap is then given by the normalized scalar product

$$\mathcal{O}[h_1, h_2] = \frac{\langle h_1 | h_2 \rangle}{\sqrt{\langle h_1 | h_1 \rangle \langle h_2 | h_2 \rangle}} \, , \qquad \mathcal{M}_{\rm best} \equiv \max_{t_A} \max_{\Phi_1} \max_{\Phi_2} \{\mathcal{O}[h_1, h_2]\} \, .$$

- That the overlap is also very high between the nonspinning binary and the binary with equal and antialigned spins, $s_0 - s_{-8}$
- The waveform from a nonspinning binary can be extremely useful across the *whole* spin diagram and yield very large overlaps even for binaries with very high spins.
- The diagonal $a_1 = -a_2$ (the u sequence) cannot be distinguished within our given numerical accuracy, whereas configurations along the diagonal $a_1 = a_2$ (the s sequence) are clearly different.

Conclusions

- Constructed a set of stable, well-posed, constraint preserving boundaries, which reduce reflection and improve accuracy for the Harmonic evolution system
- Ran a series of binary black hole configuration to cover the parameter space of aligned black hole spins and mass ratios
  - Constructed phenomenological formulae for the prediction of the spin and kick of the merger remnant
  - Kick depends quadratically on spin along $(a_1 = -a_2)$ against PN predictions
  - Quadratic fit for final spin fit from NR results and EMRI requirements
- Determined SNR for various masses and distances of binary systems from NR and PN data
- Developed analytic inspiral-merger-ringdown gravitational waveforms from black-hole (BH) binaries with non-precessing spins by matching a post-Newtonian description of the inspiral to our numerical calculations, we obtain a waveform family with a conveniently small number of physical parameters

Thank You.

Wave extraction

- It has become standard to measure waves as expansions of the Newman-Penrose Ψ_4 scalar.
- An independent method measures gage-invariant perturbations of a Schwarzschild black hole.
- 'Observers' are placed on a 2-sphere at some large radius.
- Measure odd-parity ($Q^{\times}_{lm}$) and even-parity (Q^{+}_{lm}) perturbations of the background metric.

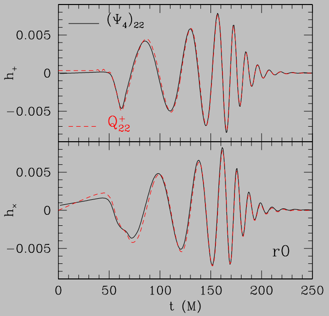

$$h_+ - \mathrm{i} h_\times = \frac{1}{\sqrt{2}r} \sum_{\ell=2}^{\infty} \sum_{m=0}^{\ell} \left(Q^+_{\ell m} - \mathrm{i} \int_{-\infty}^{t} Q^\times_{\ell m}(t')dt' \right) {}_{-2}Y^{\ell m} ,$$

Constraint Damping

- The constraint equations are the generalized harmonic coordinate conditions: $C^{\mu} \equiv \Gamma^{\mu} - \widehat{\Gamma}^{\mu} = 0$
- constraint adjustment is done by the term

$$A^{\mu\nu} = C^{\rho} A^{\mu\nu}_{\rho} \left(x^{\alpha}, g_{\alpha\beta}, \partial_{\gamma} g_{\alpha\beta}\right)$$

in the evolution equations

$$\partial_{\alpha}\left(g^{\alpha\beta}\partial_{\beta}\tilde{g}^{\mu\nu}\right) + S^{\mu\nu}\left(g, \partial g\right) + \sqrt{-g}A^{\mu\nu}$$

$$+2\sqrt{-g}\nabla^{(\mu}F^{\nu)} - \tilde{g}^{\mu\nu}\nabla_{\alpha}F^{\alpha} = 0.$$

- Dissipation: $\dot{f} \longrightarrow \dot{f} + \epsilon(\delta^{ij}D_{+i}D_{-i})w(\delta^{ij}D_{+i}D_{-i})f$ where w is a weight factor that vanishes at the outer boundary. With $D_{+i}D_{-i}$ from blended SBP stencils.

HarmonicExcision

$\left(n^i D_{+i}\right)^3 \dot{f} = 0$ to all guard points, in layers stratified by length of the outward normal pointing vector, from out to in.

LegoExcision with excision coefficients $\dfrac{x^\mu}{r}$ extrapolated around a smooth virtual surface for the inner boundary.

Radiation outer boundary conditions (i.e. outgoing only).

AEIHarmonic Evolution

- We define the evolution variables $\tilde{g}^{\mu\nu} \equiv \sqrt{-g} g^{\mu\nu}$ and $Q^{\mu\nu} \equiv n^\rho \partial_\rho \tilde{g}^{\alpha\beta}$, where n^ρ is timelike.
- This simplifies the constraint equations to

$$C^\mu \equiv -\frac{1}{\sqrt{-g}} \partial_\alpha \tilde{g}^{\alpha\mu} - \widehat{\Gamma}^\mu$$

- The AEIHarmonic code implements the first order in time system:

$$\partial_t \tilde{g}^{\mu\nu} = -\frac{g^{it}}{g^{tt}} \partial_i \tilde{g}^{\mu\nu} + \frac{1}{g^{tt}} Q^{\mu\nu}$$

$$\partial_t Q^{\mu\nu} = -\partial_i \left(\left(g^{ij} - \frac{g^{it} g^{jt}}{g^{tt}} \right) \partial_j \tilde{g}^{\mu\nu} \right) - \partial_i \left(\frac{g^{it}}{g^{tt}} Q^{\mu\nu} \right) + \tilde{S}^{\mu\nu}$$

3+1 decomposition of Einstein equations

- Foliate $\mathcal{M}$ with a set of spacelike 3-D hypersurfaces Σ_t, parametrised by t.
- Decompose the trajectories of t into components normal and parallel to Σ_t

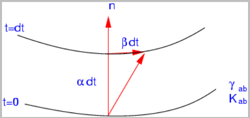

$$t^\mu = \alpha n^\mu + \beta^\mu$$

- α is called the "lapse", and fixes the distance between successive slices.
- β^μ is the "shift", and defines how coordinates move within the slice.
- These quantities are entirely gauge, ie. can be freely chosen, do not influence the physics.
- 3+1 line element:

$$ds^2 = -\alpha^2 dt^2 + \gamma_{ij}(dx^i + \beta^i dt)(dx^j + \beta^j dt).$$

3+1 decomposition of Einstein equations

- The choice of normal n^α naturally induces a metric on each slice via:

$$\gamma_{\alpha\beta} = g_{\alpha\beta} + n_\alpha n_\beta$$

- The mixed form of $\gamma_{\alpha\beta}$ projects tensors onto the spacelike hypersurfaces:

$$\perp^\alpha{}_\beta = \delta^\alpha{}_\beta + n^\alpha n_\beta$$

- Associated compatible covariant derivative in slices

$$D_\alpha := \perp^\mu{}_\alpha \nabla_\mu,$$

$$D_\alpha \gamma_{\beta\gamma} = 0.$$

- The extrinsic curvature (describing the embedding of Σ in $\mathcal{M}$) is given by:

$$K_{\alpha\beta} = - \perp_\alpha{}^\mu \perp_\beta{}^\nu \nabla_{(\mu} n_{\nu)} = -\frac{1}{2}\mathcal{L}_{\mathbf{n}}\gamma_{\alpha\beta}$$

3+1 decomposition of Einstein equations

- The 4D Einstein equations can be written out explicitly in terms of derivatives of the spatial metric and the extrinsic curvature.
  Evolution equations (6+6):

$$(\partial_t - \mathcal{L}_\beta)\gamma_{ab} = -2\alpha K_{ab}$$

$$(\partial_t - \mathcal{L}_\beta)K_{ab} = -\nabla_a \nabla_b \alpha + \alpha(R_{ab} + KK_{ab} - 2K_{ai}K^i{}_b)$$

  Constraints (1+3):

$$\mathcal{H} = R + K^2 - K_{ij}K^{ij} = 0 \qquad \text{(hamiltonian)}$$

$$\mathcal{M}_a = \nabla^i(K_{ai} - \gamma_{ai}K) = 0 \qquad \text{(momentum)}$$

- Cauchy problem for the ADM formulation of Einstein's equations:
  - Prescribe $\{\gamma_{ab}, K_{ab}\}$ at $t = 0$ subject to the constraints,
  - Specify coordinates via α and β^a,
  - Evolve data to future using Einstein eqs and definition of K_{ab}.

Evolution equations: “BSSN” Formulation

(Kojima, Nakamura, Oohara 1987, Shibata, Nakamura 1995, Baumgarte, Shapiro 1999)

Key idea: Reformulate ADM by changing variables according to certain geometrical and stability criteria.

1. Conformally decompose the 3-metric:

$$\tilde{\gamma}_{ab} = e^{-4\phi}\gamma_{ab}$$

Introduce the conformal factor as an evolution variable, and subject to the algebraic constraint $\det \tilde{\gamma}_{ab} = 1$

2. Evolve the trace of the extrinsic curvature as a separate variable.

$$\phi = \frac{1}{4}\log\psi \qquad \tilde{\gamma}_{ab} = e^{-4\phi}\gamma_{ab}$$

$$K = \gamma^{ij}K_{ij} \qquad \tilde{A}_{ab} = e^{-4\phi}(K_{ab} - \frac{1}{3}\gamma_{ab}K)$$

3. Introduce evolution variables (gauge source functions):

$$\tilde{\Gamma}^a = \tilde{\gamma}^{ij}\tilde{\Gamma}^a_{ij} = -\partial_i\tilde{\gamma}^{ai}$$

Initial data for binary black holes

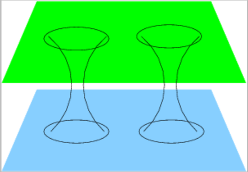

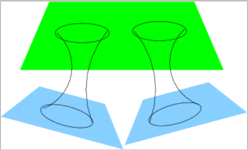

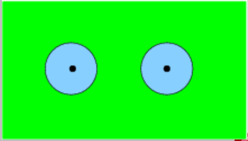

Misner data:

Two isometric, time symmetric, conformally flat, sheets connected by N black holes, solved as infinite series expansion.

Brill-Lindquist:

Conformally flat, time symmetric, hamiltonian constraint solved by:

$$\psi = 1 + \Sigma_{i=1}^{N} \frac{m_i}{2r_i}.$$

Puncture:

Assume a conformal factor of the form:

$$\psi = u + \Sigma_{i=1}^{N} \frac{m_i}{2r_i}.$$

Find C^2 solutions for u of the hamiltonian constraint:

$$\tilde{\nabla}^2 u + \frac{1}{8}\chi^7 \tilde{A}_{ij}\tilde{A}^{ij}(1+\chi u)^{-7} = 0$$